arXiv:2107.02716v2 [cs.LG] 15 Jul 2021

Evaluating subgroup disparity using epistemic uncertainty in mammography

Charles Lu [1] **Andreanne Lemay** [1] **Katharina Hoebel** [1 2] **Jayashree Kalpathy-Cramer** [1]

Abstract

As machine learning (ML) continue to be integrated into healthcare systems that affect clinical decision making, new strategies will need to be incorporated in order to effectively detect and evaluate subgroup disparities to ensure accountability and generalizability in clinical workflows. In this paper, we explore how epistemic uncertainty can be used to evaluate disparity in patient demographics (race) and data acquisition (scanner) subgroups for breast density assessment on a dataset of 108,190 mammograms collected from 33 clinical sites. Our results show that even if aggregate performance is comparable, the choice of uncertainty quantification metric can significantly the subgroup level. We hope this analysis can promote further work on how uncertainty can be leveraged to increase transparency of machine learning applications for clinical deployment.

1. Introduction

Machine learning holds tremendous promise for applications in healthcare yet real world deployment remains challenging due to difficulties in developing robust and interpretable models suitable for integration into existing clinical systems. Issues of algorithmic bias in ML have been extensively studied, several formal definitions of fairness proposed (Louizos et al., 2016; Hardt et al., 2016; Kusner et al., 2017). Previous works demonstrates how proxy variables and black box models can exacerbate biases in several different healthcare applications (Buolamwini & Gebru, 2018; Chen et al., 2019; Obermeyer et al., 2019; Larrazabal et al., 2020; Seyyed-Kalantari et al., 2020). The potential for learning systems to significantly increase disparity in protected subgroups would be a major limitation to widespread deployment of ML into critical clinical infrastructure (Du et al., 2020).

[1]Massachusetts General Hospital [2]Massachusetts Institute of Technology. Correspondence to: Charles Lu <clu@mgh.harvard.edu>.

Workshop on Interpretable ML in Healthcare at International Conference on Machine Learning (ICML). Copyright 2021 by the author(s).

For ML to be adopted in healthcare, new strategies and perspectives will need to be developed and incorporated to better monitor and audit algorithmic-assisted workflows for robustness and transparency. Inspired by works, such as Bhatt et al. (2020), which advocates for the use of uncertainty as one approach to achieve more transparency in ML, and Dusenberry et al. (2020), which shows ML model exhibiting higher uncertainty for different demographics in electronic health records, we investigate how uncertainty could be used to detect and evaluate disparities between subgroups. Subgroup analysis is important in many clinical settings, especially in non-stationary distributions where characteristics of data acquisition change over time (e.g. clinical equipment is upgraded or protocols are changed)(Ghassemi et al., 2018). The integration of predictive uncertainty can have implications for both regulation and generalizability of machine learning applications in healthcare by allowing clinicians more easily interpret predictions, investigate possible failure modes, and adjust safety thresholds according to different clinical contexts. Incorporating uncertainty thresholds into clinical ML workflows can be set to abnormal and ambiguous cases for manual review and to monitor how models behave under distribution shifts or on subgroups with different base rates. Uncertainty modeling can be broadly categorized into *epistemic* (model uncertainty) and *aleatoric* (data uncertainty)(Kiureghian & Ditlevsen, 2009). Epistemic uncertainty is important in many data-limited and safety-critical applications, such as medical image analysis, and can indicate poor generalizability (Kendall & Gal, 2017; DeVries & Taylor, 2018).

Popular Bayesian approximation methods used to assess epistemic uncertainty include Deep Ensembles (Lakshminarayanan et al., 2017) and Monte Carlo (MC) Dropout (Gal & Uk, 2016). Leibig et al. (2017) showed excluding samples with high uncertainty, which could be referred later for additional followup and review, overall performance improved in diabetic retinopathy screening. Similarly, in the classification of dermoscopic images, epistemic uncertainty was higher for misclassified and out-of-distribution data (Combalia et al., 2020).

In this paper, we evaluate several common forms of uncertainty quantification (UQ) on a large, heterogeneous mammography dataset for breast density assessment and propose a novel disparity metric based on epistemic uncertainty to

show how disparities manifest in racial demographics and scanner acquisition subgroups. This metric may be useful in characterizing failure modes or detecting distribution shift.

2. Methods

2.1. Measures of uncertainty quantification

We use Monte Carlo dropout (Gal & Uk, 2016) as a Bayesian approximation to epistemic uncertainty to sample T softmax probabilities, $\{p_t\}_{t=1}^{T} = p_1, p_2, \ldots, p_t$, which are averaged along the class dimension for the final prediction, $\hat{y} = \arg\max_C \frac{1}{T}\sum_{t=1}^{T} p_{t|c}$. We compare the following uncertainty metrics: maximum softmax probability, predictive variance, predicted entropy, and Bhattacharyya coefficient.

As detailed in Hendrycks & Gimpel (2017) to detect out-of-distribution examples, we use maximum softmax probability (Naive) as our baseline uncertainty.

$$\text{Naive}(p) = 1 - \max(p) \tag{1}$$

Predictive variance is defined as the average variance computed over T MC samples

$$\text{Var}\left(\{p\}_{t=1}^{T}\right) = \frac{1}{C}\sum_{c=1}^{C}\text{Var}(p_c) \tag{2}$$

where $Var(p_c) = \frac{1}{T}\sum_{t=1}^{T}\left(p_{t|c} - \frac{1}{T}\sum_{t=1}^{T} p_{t|c}]\right)^2$.

Predictive entropy the expected information over T MC samples

$$\text{H}\left(\{p\}_{t=1}^{T}\right) = -\frac{1}{C}\sum_{c=1}^{C}\left(\frac{1}{T}\sum_{t=1}^{T} p_{t|c}\log\frac{1}{T}\sum_{t=1}^{T} p_{t|c}\right) \tag{3}$$

Bhattacharyya coefficient (BC) is a measure of similarity between two samples. In this case, we compute BC using N-bin histogram of the top two classes, $h^1 = \text{histogram}(\{p_{c=c_1}\}_{t=1}^{T}$ and $h^2 = \text{histogram}(\{p_{c=c_2}\}_{t=1}^{T}$, as determined by their predictive mean.

$$\text{BC}\left(\{p\}_{t=1}^{T}\right) = \frac{1}{N}\sum_{n=1}^{N}\sqrt{h_n^1 h_n^2} \tag{4}$$

Subsequently, given some measure of uncertainty quantification UQ, a performance metric $\text{PM}(\hat{Y}, Y)$, a set of rejection thresholds, $\{r\}_{i=1}^{n} = r_1, r_2, \ldots, r_n$, and a mutually exclusive subgroup attribute, $\mathcal{A}$, such as patient race or scanner model, we can define the following subgroup disparity metric

$$\delta = \frac{1}{n}\sum_{i=1}^{n}\sum_{A,A'\in\binom{\mathcal{A}}{2}}\left|f(r_i, A) - f(r_i, A')\right| \tag{5}$$

where $\binom{\mathcal{A}}{2}$ is the set of unique pairwise subgroups and $f = \text{PM}\left(\{\hat{y}\in\hat{Y} \mid A,\ \text{UQ}(\hat{y}) < r_i\}, \{y\in Y \mid A,\ \text{UQ}(\hat{y}) < r_i\}\right)$ is the performance on subgroup A at threshold r_i.

2.2. Dataset

We perform all experiments on the Digital Mammographic Imaging Screening Trial (DMIST) dataset, which comprises 108,230 mammograms from 21,729 patients from 33 clinical sites and interpreted by a total of 92 radiologists (Pisano et al., 2005). Accurate assessment of breast density, as measured by relative amounts of fibroglandular tissue, is important for the interpretation of mammographies and is commonly rated according to the BI-RADS criteria into one of four categories: entirely fatty, scattered, heterogeneously dense, and extremely dense (Liberman & Menell, 2002).

2.3. Experiments

To assess the performance of breast density task, we use linearly weighted Cohen's Kappa score, $\kappa \in [-1, 1]$, which is commonly used to measure agreement between two raters, where P_o is the proportion of observed agreement and P_e is the agreement to due random chance (McHugh, 2012).

$$\kappa = \frac{P_o - P_e}{1 - P_e} \tag{6}$$

We consider two subgroups to analyze on a patient level: 5 races (white, black, hispanic, asian, and other) and and 4 scanner types (Senograph, Senscan, ADS, and other).

We split the DMIST dataset by patients into a held-out test set of 38,936 (35.9%) mammograms and a development set of 69,254 mammograms, which was further split randomly into training and validation sets (90% / 10% respectively). All experiments used the ResNet50 (He et al., 2016) architecture with dropout layers ($p = 0.1$), implemented using the MONAI framework (Ma et al., 2021), finetuned from ImageNet (Russakovsky et al., 2015), and trained with cross-entropy loss using the ADAM optimizer for up to 100 epochs with early stopping using patience of 5 epochs. Random data augmentation in rotations, flipping, resizes, affine transforms, and cropping was applied during training.

Each experiment was performed five times with different random seeds. To estimate uncertainty, 100 Monte Carlo predictions were sampled for each test image and final predictions were obtained by averaging over all samples. Finally, predictions from distinct mammograms of the same patient were averaged to obtain patient level predictions.

3. Results

The overall Kappa score on our test set was 0.646 ± 0.016. Unsurprisingly, performance is highest for the most repre-

sented subgroups in the data distribution: 0.647 ± 0.015 for white patients and 0.658 ± 0.021 Senograph scanners (Table 1). Comparing within subgroups, we do not find any significant relationship between uncertainty and race and a moderate relationship between number of examples and uncertainty for acquisition type (Table 1). For breast density, there is a strong negative correlation between class proportion and uncertainty, with scattered and heterogeneous having lower uncertainty than fatty and dense classes (Table 1).

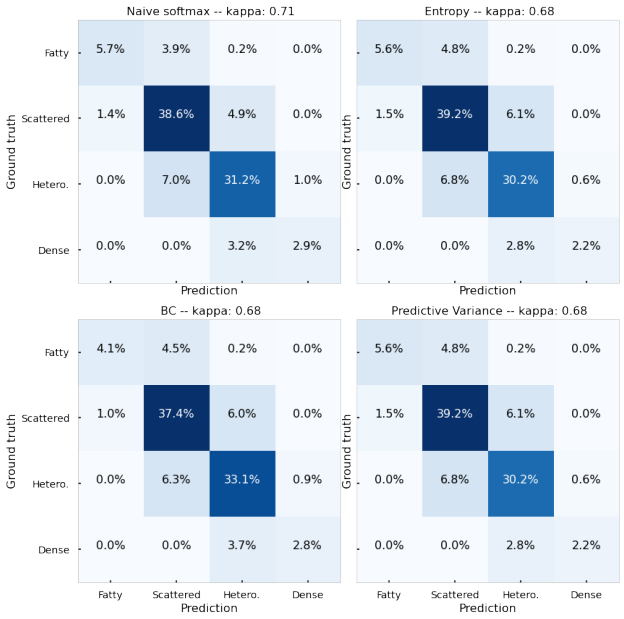


Figure 1. Confusion matrix of four types of uncertainty measures (maximum softmax probability, predictive entropy, Bhattacharyya coefficient, and predictive variance) at 20% uncertainty threshold

As shown in Figure 1, aggregate Kappa score is comparable between uncertainty metrics with similar distribution of breast density ratings at 20% uncertainty threshold. However, when analyzing at subgroup level, we observe that predictive variance has significantly lower disparity for both race and scanner categories (Figures 2 - 3 and Table 2). In Figure 2, we see increasing trend in subgroup disparity, even as overall performance improves as more uncertain cases are rejected, with predictive variance remaining the most stable across the range of considered rejection thresholds. For scanner subgroups in Figure 3, we observe that predictive entropy and predictive variance to be relatively stable for low uncertainty thresholds and predictive variance significantly decreasing in disparity at higher thresholds 25%. The race and acquisition disparities at different rejection thresholds are also listed in Table 2. Further examining the difference in Kappa scores between scanner acquisition types in Figure 4, we observe that predictive variance performed especially well on the least represented scanner type.

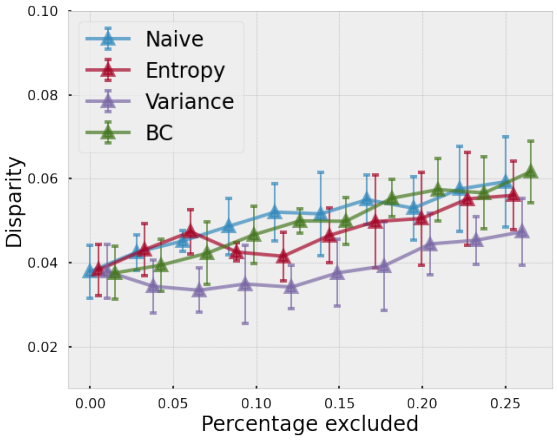


Figure 2. Average Kappa disparity between race subgroup as uncertainty threshold increases (lower disparity is better).

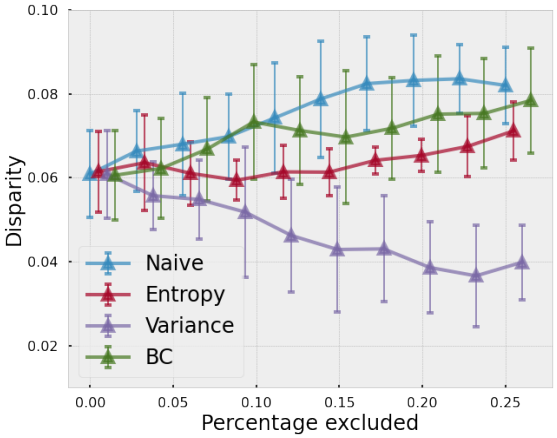


Figure 3. Average Kappa disparity between scanner subgroup as uncertainty threshold increases (lower disparity is better).

4. Conclusion

In this work, we proposed a simple evaluation strategy to analyze subgroup disparities to compare different measures of epistemic uncertainty. Our experiments on a large dataset of mammograms demonstrate how the choice of uncertainty metric can disproportionately affect subgroups, such as race and scanner, even when aggregate performance appear similar. We find that using predictive variance for uncertainty maintained the lowest level of disparity in both race and

Table 1. Performance (mean ± std), subgroup disparity, and distribution by subgroup (race, scanner, label). Note that kappa score is not well defined on a single class label for breast density subgroups.

	κ	NAIVE	VAR. ($\times 10^{-3}$)	ENTR.	BC	DISTRIBUTION
Race						
WHITE	**0.647 ± 0.015**	0.287 ± 0.004	**3.5 ± 0.2**	**0.172 ± 0.003**	0.808 ± 0.005	80.7%
BLACK	0.641 ± 0.019	0.292 ± 0.004	3.9 ± 0.3	0.173 ± 0.003	0.808 ± 0.004	13.1%
HISP.	0.573 ± 0.020	**0.285 ± 0.007**	4.3± 0.4	0.175 ± 0.006	**0.795 ± 0.010**	3.7%
ASIAN	0.627 ± 0.042	0.296 ± 0.006	**3.5± 0.2**	0.180 ± 0.004	0.809 ± 0.009	1.8%
OTHER	0.625 ± 0.031	0.286 ± 0.007	3.7± 0.1	0.174 ± 0.003	**0.795 ± 0.010**	0.7%
Acquisition type						
SENOGRAPH	**0.658 ± 0.021**	0.280 ± 0.004	3.4 ± 0.3	0.166 ± 0.003	0.801 ± 0.004	55.8%
SENOSCAN	0.641 ± 0.011	0.304 ± 0.005	3.7 ± 0.2	0.183 ± 0.003	0.822 ± 0.007	36.4%
ADS	0.599 ± 0.024	0.272 ± 0.005	**3.2 ± 0.3**	**0.164 ± 0.004**	0.793 ± 0.003	5.4%
OTHER	0.551 ± 0.025	**0.270 ± 0.012**	5.9 ± 0.5	0.174 ± 0.010	**0.764 ± 0.018**	2.5%
Breast density						
FATTY	N/A	0.301 ± 0.008	4.3 ± 0.6	0.172 ± 0.002	0.840 ± 0.011	10.8%
SCATTERED	N/A	**0.279 ± 0.008**	**3.3 ± 0.3**	**0.171 ± 0.004**	0.805 ± 0.008	43.2%
HETEROGENEOUS	N/A	0.291 ± 0.008	3.4 ± 0.2	0.173 ± 0.004	**0.801 ± 0.006**	38.9%
DENSE	N/A	0.307 ± 0.011	5.0 ± 0.4	0.178 ± 0.006	0.806 ± 0.012	7.1%
OVERALL	0.646 ± 0.016	0.288 ± 0.004	3.6 ± 0.2	0.172 ± 0.003	0.807 ± 0.004	

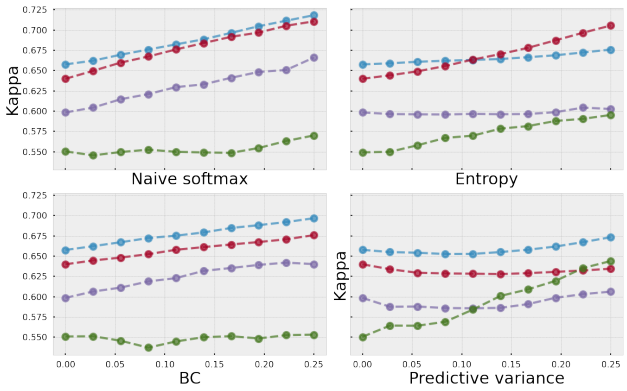


Figure 4. Comparison of uncertainty performance by acquisition scanner type (blue is Senograph; red is Senoscan; purple is ADS; green is Other)

scanner subgroups at different rejection thresholds. Interestingly, disparity in scanner actually decreased substantially at higher thresholds with predictive variance. Future work might explore subgroup uncertainty in other clinical datasets as well as evaluating other definitions of uncertainty in healthcare contexts. Additionally, human reader studies will be crucial in investigating how clinical users interface with uncertainty estimates in different contexts to make a decision.

Table 2. Change in disparity (mean ± std) by uncertainty metric for racial and acquisition subgroups at different rejection thresholds.

	PROPORTION OF EXCLUDED CASES		
	1%	**10%**	**25%**
Race disparity			
NAIVE	0.041 ± 0.005	0.051 ± 0.007	0.059 ± 0.011
VAR.	0.037 ± 0.008	0.034 ± 0.007	0.047 ± 0.008
ENTR.	0.040 ± 0.007	0.040 ± 0.004	0.056 ± 0.008
BC	0.038 ± 0.005	0.048 ± 0.003	0.062 ± 0.007
Acquisition disparity			
NAIVE	0.064 ± 0.010	0.073 ± 0.013	0.082 ± 0.009
VAR.	0.061 ± 0.012	0.050 ± 0.015	0.040 ± 0.009
ENTR.	0.063 ± 0.011	0.062 ± 0.006	0.071 ± 0.007
BC	0.061 ± 0.012	0.070 ± 0.013	0.078 ± 0.012
KAPPA κ	0.646 ± 0.001	0.657 ± 0.012	0.682 ± 0.019

References

Bhatt, U., Antorán, J., Zhang, Y., Liao, Q. V., Sattigeri, P., Fogliato, R., Melançon, G. G., Krishnan, R., Stanley, J., Tickoo, O., Nachman, L., Chunara, R., Srikumar, M., Weller, A., and Xiang, A. Uncertainty as a Form of Transparency: Measuring, Communicating, and Using Uncertainty. 2020. URL http://arxiv.org/abs/2011.07586.

Buolamwini, J. and Gebru, T. Gender Shades: Intersectional

Accuracy Disparities in Commercial Gender Classification. *Conference proceedings: Conference on Fairness, Accountability, and Transparency*, 2018. ISSN 11786930. doi: 10.2147/OTT.S126905.

Chen, I., Szolovits, P., and Ghassemi, M. Can AI Help Reduce Disparities in General Medical and Mental Health Care? *AMA Journal of Ethics*, 21(2):167–179, 2019.

Combalia, M., Hueto, F., Puig, S., Malvehy, J., and Vilaplana, V. Uncertainty estimation in deep neural networks for dermoscopic image classification. In *IEEE Computer Society Conference on Computer Vision and Pattern Recognition Workshops*, volume 2020-June, pp. 3211–3220, 2020. ISBN 9781728193601. doi: 10.1109/CVPRW50498.2020.00380. URL https://openaccess.thecvf.com/content_CVPRW_2020/papers/w42/Combalia_Uncertainty_Estimation_in_Deep_Neural_Networks_for_Dermoscopic_Image_Classification_CVPRW_2020_paper.pdf.

DeVries, T. and Taylor, G. W. Leveraging Uncertainty Estimates for Predicting Segmentation Quality. 2018. URL http://arxiv.org/abs/1807.00502.

Du, M., Yang, F., Zou, N., and Hu, X. Fairness in Deep Learning: A Computational Perspective. *IEEE Intelligent Systems*, pp. 1–9, 2020. ISSN 19411294. doi: 10.1109/MIS.2020.3000681.

Dusenberry, M. W., Tran, D., Choi, E., Kemp, J., Nixon, J., Jerfel, G., Heller, K., and Dai, A. M. Analyzing the role of model uncertainty for electronic health records. *ACM CHIL 2020 - Proceedings of the 2020 ACM Conference on Health, Inference, and Learning*, pp. 204–213, 2020. doi: 10.1145/3368555.3384457.

Gal, Y. and Uk, Z. A. Dropout as a Bayesian Approximation: Representing Model Uncertainty in Deep Learning Zoubin Ghahramani. Technical report, 6 2016. URL http://yarin.co.

Ghassemi, M., Naumann, T., Schulam, P., Beam, A. L., and Ranganath, R. Opportunities in machine learning for healthcare. *CoRR*, abs/1806.00388, 2018. URL http://arxiv.org/abs/1806.00388.

Hardt, M., Price, E., Price, E., and Srebro, N. Equality of opportunity in supervised learning. In Lee, D., Sugiyama, M., Luxburg, U., Guyon, I., and Garnett, R. (eds.), *Advances in Neural Information Processing Systems*, volume 29. Curran Associates, Inc., 2016. URL https://proceedings.neurips.cc/paper/2016/file/9d2682367c3935defcb1f9e247a97c0d-Paper.pdf.

He, K., Zhang, X., Ren, S., and Sun, J. Deep residual learning for image recognition. In *Proceedings of the IEEE Computer Society Conference on Computer Vision and Pattern Recognition*, volume 2016-December, pp. 770–778. IEEE Computer Society, 12 2016. ISBN 9781467388504. doi: 10.1109/CVPR.2016.90.

Hendrycks, D. and Gimpel, K. A baseline for detecting misclassified and out-of-distribution examples in neural networks. *Proceedings of International Conference on Learning Representations*, 2017.

Kendall, A. and Gal, Y. What uncertainties do we need in Bayesian deep learning for computer vision? In *Advances in Neural Information Processing Systems*, volume 2017-Decem, pp. 5575–5585, 3 2017. URL http://arxiv.org/abs/1703.04977.

Kiureghian, A. D. and Ditlevsen, O. Aleatory or epistemic? Does it matter? *Structural Safety*, 31(2):105–112, 3 2009. ISSN 01674730. doi: 10.1016/j.strusafe.2008.06.020.

Kusner, M. J., Loftus, J., Russell, C., and Silva, R. Counterfactual fairness. In Guyon, I., Luxburg, U. V., Bengio, S., Wallach, H., Fergus, R., Vishwanathan, S., and Garnett, R. (eds.), *Advances in Neural Information Processing Systems*, volume 30. Curran Associates, Inc., 2017. URL https://proceedings.neurips.cc/paper/2017/file/a486cd07e4ac3d270571622f4f316ec5-Paper.pdf.

Lakshminarayanan, B., Pritzel, A., and Deepmind, C. B. Simple and Scalable Predictive Uncertainty Estimation using Deep Ensembles. Technical report, 2017.

Larrazabal, A. J., Nieto, N., Peterson, V., Milone, D. H., and Ferrante, E. Gender imbalance in medical imaging datasets produces biased classifiers for computer-aided diagnosis. *Proceedings of the National Academy of Sciences of the United States of America*, 117(23):12592–12594, 2020. ISSN 10916490. doi: 10.1073/pnas.1919012117.

Leibig, C., Allken, V., Ayhan, M. S., Berens, P., and Wahl, S. Leveraging uncertainty information from deep neural networks for disease detection. *Scientific Reports*, 7(1):17816, 12 2017. ISSN 20452322. doi: 10.1038/s41598-017-17876-z. URL http://www.nature.com/articles/s41598-017-17876-z.

Liberman, L. and Menell, J. H. Breast imaging reporting and data system (bi-rads). *Radiologic clinics of North America*, 40:409–430, 3 2002. doi: 10.1016/s0033-8389(01)00017-3.

Louizos, C., Swersky, K., Li, Y., Welling, M., and Zemel, R. S. The variational fair autoencoder. In *ICLR*, 2016. URL http://arxiv.org/abs/1511.00830.

Ma, N., Li, W., Brown, R., Wang, Y., Behrooz, Gorman, B., Johnson, H., Yang, I., Kerfoot, E., charliebudd, Li, Y., Adil, Mohammad, Y.-T. H., Aggarwal, A., Trentz, C., aji, a., masadcv, Graham, M., Murray, B., Daroach, G., Tudosiu, P.-D., myron, McCormick, M., Ambros, Balamurali, Baker, C., Sellner, J., Fidon, L., and cgrain. Project-MONAI/MONAI: 0.5.3. 6 2021. doi: 10.5281/ZENODO.4891800. URL https://zenodo.org/record/4891800.

McHugh, M. L. Interrater reliability: the kappa statistic. *Biochemia medica*, 22:276–282, 3 2012.

Obermeyer, Z., Powers, B., Vogeli, C., and Mullainathan, S. Dissecting racial bias in an algorithm used to manage the health of populations. *Science*, 366(6464):447–453, 2019. ISSN 0036-8075. doi: 10.1126/science.aax2342. URL https://science.sciencemag.org/content/366/6464/447.

Pisano, E. D., Gatsonis, C., Hendrick, E., Yaffe, M., Baum, J. K., Acharyya, S., Conant, E. F., Fajardo, L. L., Bassett, L., D'Orsi, C., Jong, R., and Rebner, M. Diagnostic Performance of Digital versus Film Mammography for Breast-Cancer Screening. *New England Journal of Medicine*, 353(17):1773–1783, 10 2005. ISSN 0028-4793. doi: 10.1056/NEJMoa052911. URL http://www.nejm.org/doi/abs/10.1056/NEJMoa052911.

Russakovsky, O., Deng, J., Su, H., Krause, J., Satheesh, S., Ma, S., Huang, Z., Karpathy, A., Khosla, A., Bernstein, M., Berg, A. C., and Fei-Fei, L. ImageNet Large Scale Visual Recognition Challenge. *International Journal of Computer Vision*, 115(3):211–252, 12 2015. ISSN 15731405. doi: 10.1007/s11263-015-0816-y. URL http://image-net.org/challenges/LSVRC/.

Seyyed-Kalantari, L., Liu, G., McDermott, M., Chen, I. Y., and Ghassemi, M. CheXclusion: Fairness gaps in deep chest X-ray classifiers. *arXiv e-prints*, art. arXiv:2003.00827, February 2020.